ARTICLE

Methanol Adsorption on TiO_2 Film Studied by Sum Frequency Generation Vibrational Spectroscopy

Ran-ran Feng[a,b†], An-an Liu[a,b†], Shuo Liu[a,b], Jiao-jian Shi[a,b], Yi Liu[a,b], Ze-feng Ren[a,b*]

a. International Center for Quantum Materials (ICQM) and School of Physics, Peking University, Beijing 100871, China
b. Collaborative Innovation Center of Quantum Matter, Beijing 100871, China

(Dated: Received on September 16, 2014; Accepted on October 20, 2014)

A broadband infrared surface sum frequency generation vibrational spectroscopy (SFG-VS) and an *in situ* UV excitation setup devoted to studying surface photocatalysis have been constructed. With a home-made compact high vacuum cell, organic contaminants on TiO_2 thin film surface prepared by RF magnetron sputtering were *in situ* removed under 266 nm irradiation in 10 kPa O_2 atmosphere. We obtained the methanol spectrum in the CH_3 stretching vibration region on TiO_2 surface with changing the methanol pressure at room temperature. Features of both molecular and dissociative methanol, methoxy, adsorbed on this surface were resolved. The CH_3 symmetric stretching vibration frequency and Fermi resonance of molecular methanol is red-shifted by about $6-8$ cm^{-1} from low to high coverage. Moreover, the recombination of dissociative methanol and H on surfaces in vacuum was also observed. Our results suggest two equilibria exist: between molecular methanol in the gas phase and that on surfaces, and between molecular methanol and dissociative methanol on surfaces.

Key words: Surface sum frequency generation vibrational spectroscopy, Surface photocatalysis, TiO_2

I. INTRODUCTION

Since the first report of UV-induced redox chemistry on TiO_2 [1], TiO_2 has attracted extensive attention due to its wide applications in the areas of air purification, waste water treatment, self-cleaning glass and so on, especially in the last decade. Recently, the understanding of adsorption structure and photochemistry of organic molecules on TiO_2 has made much progress on the molecular level [2–7].

Methanol, as the simplest alcohol, has been thoroughly studied on $TiO_2(110)$ surfaces as a model molecule of photooxidation of organic contaminants. Henderson and co-workers conducted a detailed study of thermal reaction of CH_3OH on $TiO_2(110)$ using variant surface chemistry techniques, and concluded that the majority of the CH_3OH molecules were adsorbed on 5-coordinated Ti sites, and CH_3OH adsorbed on bridge-bonded oxygen vacancy sites dissociated to methoxy and H on bridged-bonded oxygen sites (BBOH) [8], which was imaged by atomically resolved scanning tunneling microscopy (STM) [9]. They identified that the methoxy group was the active species in the photochemical hole scavenging reaction of methanol on $TiO_2(110)$ surfaces [10]. An excited electronic state on $CH_3OH/TiO_2(110)$ was found with two-photon photoemission spectroscopy (2PPE) [11, 12]. Yang and co-workers employed the combination of time-dependent 2PPE and STM, and found site-specific photoinduced dissociation of CH_3OH at 5-coordinated Ti sites [12]. They used a temperature dependent desorption (TPD) with laser excitation and observed a stepwise photocatalytic dissociation of CD_3OH adsorbed on 5-coordinated Ti sites to methoxy, CD_3O, and BBOH, and further to formaldehyde, CD_2O, and BBOD under 400 nm light irradiation [13]. Later, further oxidation of methanol to methyl formate was also found under UV light irradiation [14–16].

Theoretically, Yang and co-workers attributed the surface excited electronic state to a photocatalytic dissociated state of CH_3OH on $TiO_2(110)$ [12], which was different from the assignment of wet electron states of Petek and co-workers [17]. Due to the limited ability of density functional theory (DFT) on excited electronic state of surface, it's difficult to know which species and what happen under excitation on the surface from the 2PPE data [18, 19]. However, the DFT based on the ground electronic state could interpret the stepwise dissociation of methanol on TiO_2 [13].

The TPD method not only provides us the adsorption information of methanol on TiO_2 [8, 20] , but also

†These authors contributed equally to this work.
*Author to whom correspondence should be addressed. E-mail: zfren@pku.edu.cn

offers rich evidence of its photocatalytic reaction in the molecular level [13–16]. However, TPD only probes the desorption species from the heating surface, and we cannot exclude any thermal reaction when heating up the sample. The high resolution electron energy loss spectroscopy (HREELS) and low energy electron diffraction (LEED) can provide *in situ* measurements, but Henderson and co-workers showed that electrons can induce decomposition of methanol on TiO_2(110) [8, 20]. IR absorption spectroscopy is a powerful tool for identifying the species on oxide surfaces. Only a few experiments have been done on TiO_2 single crystal due to extremely low signal [21–23] while there are a large set of studies on TiO_2 powders and thin films [2]. Instead of linear IR spectroscopy, Shultz and co-workers, for the first time, employed a second-order surface sum frequency generation vibrational spectroscopy (SFG-VS), which is surface specific, to characterize the methanol and methoxy adsorption structures on anatase TiO_2 nanoparticle thin films [24, 25].

In the present work, we used a newly setup, broadband infrared SFG vibrational spectrometer, to *in situ* study methanol adsorption on TiO_2 thin film prepared by RF magnetron sputtering. We obtained the SFG spectra of CH_3OH/TiO_2 at different methanol pressure, and analyzed the SFG signal of molecular and dissociative methanol relating to the methanol pressure with global fitting.

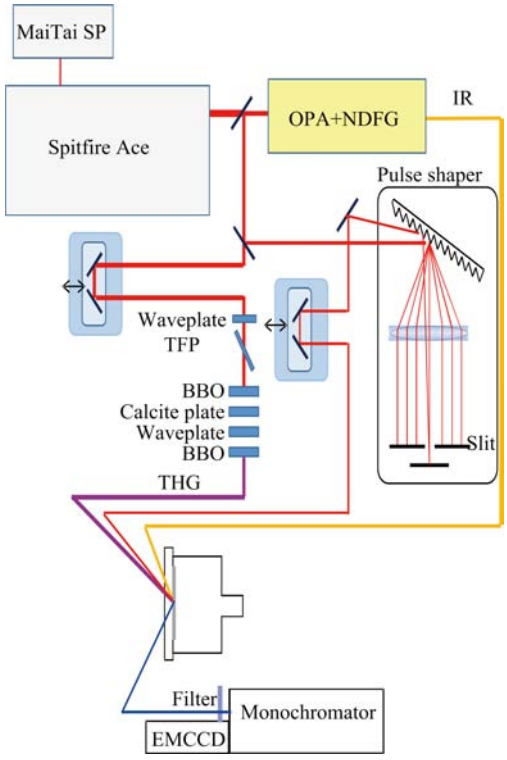

FIG. 1 A schematic of SFG light path, and a thin film sample cell.

II. EXPERIMENTS

The schematic of SFG setup is shown in Fig.1. An optical parametric amplifier (TOPAS-USF, Light Conversion) pumped by 60% power of the amplifier Ti:Sapphire laser system (Spitfire ACE, Newport, 5 mJ, 800 nm, 35 fs, 1 kHz repetition rate) generates tunable near-IR pulses (signal and idler, 1.16−2.6 μm). The mid-IR (2.6−11 μm) is subsequently generated by nonlinear difference frequency mixing (NCDFM1, Light Conversion) of signal and idler in $AgGaS_2$. The femtosecond IR pulse at about 3.4 μm wavelength is roughly 20 mW. We used a GaAs (100) surface to get the IR profile, whose apparent bandwidth is typically 240 cm^{-1} (FWHM), smaller than the real one due to the limited diameter of the visible light. 20% power from the amplifier is spectrally narrowed as the visible light (VIS) using a pulse shaper (1800 L/mm pulse compression grating, Spectrogon; cylindrical lens with 200 mm focal length), normally FWHM 7.5 cm^{-1} and 14 mW in our experiment. The residual power is used to generate the third harmonic, UV 266 nm. Second harmonic, 400 nm, is generated in a type I β-barium borate. And a calcite plate compensates the delay between the fundamental and the second harmonic, which then pass a waveplate ($\lambda/2$=800 nm, λ=400 nm) and are mixed in another type I -barium borate to generate a third harmonic. The delay of 266 nm laser is controlled by a hybrid translation stage (M-511.HD, Physik Instrumente). Typically, 30 mW UV light, tuned by combination of a waveplate and a thin film polarizer (TFP), is used in our experiment. The diameter of 266 nm laser is about 1.5 mm on the surface, which is much larger than VIS and IR laser spots to easily insure overlap.

Both polarizations of the VIS and IR are controlled by true zero-order half-wave plates, and the SFG signal polarization is selected and controlled by the combination of an achromatic half-wave plate and a Glan polarizer. The SFG signal is collimated by a lens and isolated from the VIS and IR beams by optical irises and double 775 nm shortpass filters (Semrock) right in front of a 500 mm monochromator (SP2500, Princeton Instruments) entrance slit. The SFG signal is focused onto the entrance slit, dispersed by a 1200 L/mm grating and imaged onto 5 pixels (full width) vertically of a thermoelectrically cooled (−60 °C) electron-multiplied CCD camera (Princeton Instruments, ProEM Excelon) containing a 1600×400, 16 μm^2, pixel array. Here, all SFG spectra correspond to the ssp (SF, VIS, IR) polarization combination. Our SFG system is extremely stable benefiting from the stable temperature (±0.2 °C when running laser) in the home-design clean room.

The CaF_2 substrates (25 mm in diameter, 3 mm in thickness) were soaked and ultrasonically cleaned in toluene, rinsed in deionized water and soaked in methanol, rinsed in deionized water again, dried with nitrogen gas, and finally cleaned with plasma (Harrick)

DOI:10.1063/1674-0068/28/cjcp1409154

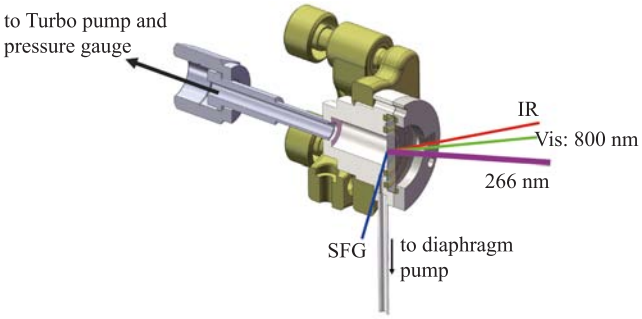

FIG. 2 The cut view of the cell and the schematic of SFG and THG light path on the TiO_2 thin film.

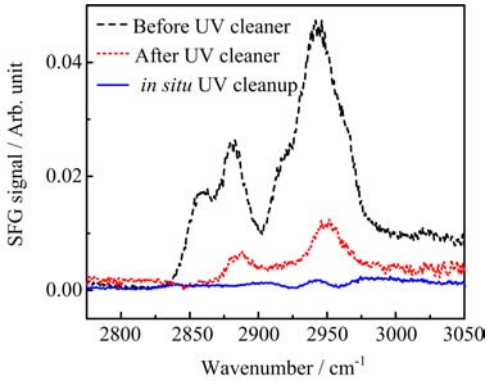

FIG. 3 SFG-VS in the CH stretching vibration region of the organic contaminants on TiO_2 thin film with UV cleaner and *in situ* 266 nm irradiation in 10 kPa O_2 atmosphere.

for 10 min. CaF_2 substrates were stored in a Teflon box before using. We prepared the TiO_2 thin film on CaF_2 substrates by RF magnetron sputtering. The working pressure of the working gas, argon, was 1 Pa, and the flow was 30 sccm. The 60 nm thick TiO_2 film was prepared with RF power 60 W for 30 min and the substrate at room temperature. This method produced the mixed phase of anatase and rutile [26]. The methanol (99.95% purity) was purified further by several freeze-pump-thaw cycles before experiment.

The CaF_2 window with TiO_2 thin film was mounted on a home-made cell, as shown in Fig.2. We used double *o*-ring sealing and differential pumping methods to avoid leakage and to achieve high vacuum condition in the cell. The ultimate pressure is less than 5×10^{-8} Torr. The absolute pressure of gas in the cell is monitored with a capacitance gauge (CPCA-330Z, Shanghai Zhentai Instruments). The whole cell is mounted on a mirror mount (Polaris, Thorlabs) and two-axis linear stages, with which SFG signal can be easily optimized. All the gas handling system is assembled by CF flanges and VCR connections, which can reduce the risk of leakage.

The SFG intensity is given by

$$I_{\mathrm{SFG}} = \left| A_{\mathrm{NR}} + \sum_q \frac{A_q e^{i\Phi_q}}{\omega_{\mathrm{IR}} - \omega_q + i\Gamma_q} \right|^2 I_{\mathrm{Vis}} I_{\mathrm{IR}} \propto N^2 \left|\langle\beta\rangle\right|^2 \quad (1)$$

where A_{NR} is nonresonance amplitude; A_q, Φ_q, ω_q, Γ_q are the amplitude, phase, resonant frequency, and damping constant (half width at half maximum) of the q-th mode, respectively; N is density of adsorbates, $\langle\beta\rangle$ is the angular average of the molecular hyperpolarizability. The measured SFG signal was normalized to the apparent IR profile ($\propto I_{\mathrm{Vis}} I_{\mathrm{IR}}$) obtained at GaAs(100) surface located at the same position of the TiO_2 thin film. Due to the limited resolution and signal-to-noise ratio and much more parameters than simple linear absorption spectra, the meaningful quantitative information is difficult to be obtained with the fitting of SFG spectra [27]. We developed a global fitting program based on Matlab software, which can fit multiple resonant frequencies of multiple curves with any algebraic relationship among fitting parameters based on SFG (Eq.(1)). And 85 parameters were reduced to 53 with setting the same phase Φ_q and damping constant Γ_q for 4 resonant terms of 5 curves.

III. RESULTS AND DISCUSSION

The newly prepared TiO_2 thin film was contaminated with organic molecules under ambient conditions. Figure 3 shows the SFG spectra in the CH stretching vibration region of TiO_2 thin film, and most contaminants were removed after UV cleaner (SAMCO's UV-1, N_2 purged). To avoid contamination under ambient conditions, we used the third harmonic, 266 nm, irradiation to *in situ* remove the contaminants with filling 10 kPa O_2 in the cell by photodegradation reaction. The typical spectrum of residual contaminants on bare surface is shown in Fig.3. Routinely, the TiO_2 surface was refreshed with 30 mW 266 nm treatment for 1 h in 10 kPa O_2 atmosphere in the cell before measurements.

Figure 4 shows the SFG-VS of methanol on TiO_2 thin film at different methanol pressures, which is similar to the results of Shultz and co-workers [24]. Based on our global fitting program, we got four resonances located at 2826 (Res 1), 2848 (Res 2), 2928 (Res 3) and 2958 cm^{-1} (Res 4) for 30 Pa CH_3OH, respectively. The fitting results are shown in the supplementary material. All the four features arise as the pressure of CH_3OH, while the second and fourth features increase more obviously. We assigned the resonances at 2826 and 2928 cm^{-1} to the symmetric stretch (ν_s) and symmetric Fermi resonance (ν_F) [28, 29] of CH_3 group of methoxy, chemically adsorbed on TiO_2, and the other two resonances at 2848 and 2958 cm^{-1} to that of molecular methanol, physically adsorbed on TiO_2 [24]. As increasing the methanol pressure to 4 kPa, the first and third resonant frequencies almost keep invariant, while

DOI:10.1063/1674-0068/28/cjcp1409154

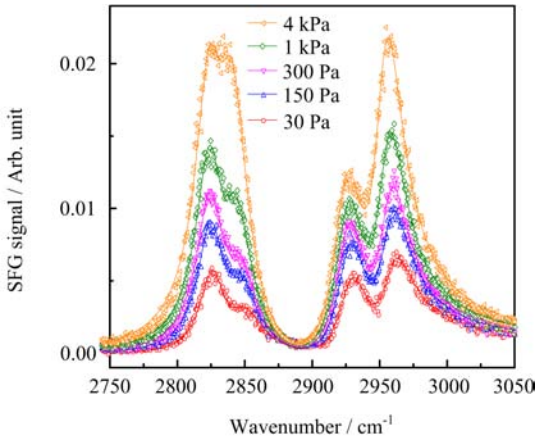

FIG. 4 SFG spectra (dot) of methanol on TiO_2 thin film as a function of methanol pressure and their global fittings (line).

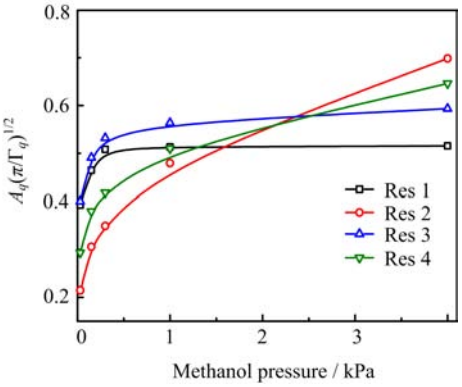

FIG. 5 Densities of methoxy and methanol on TiO_2 *vs.* methanol pressure in the cell.

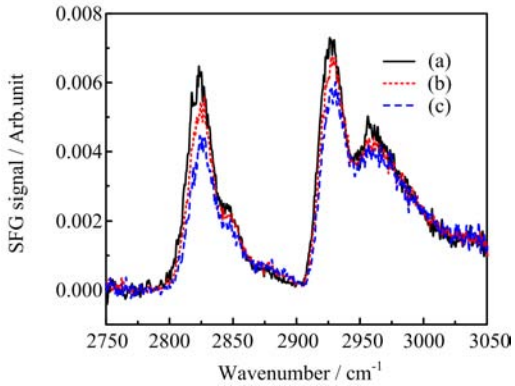

FIG. 6 The methoxy signal as a function of pumping time. 300 Pa CH_3OH is filled in the cell before pumping. (a) Evacuation for 3 min, $<4\times10^{-6}$ Torr, (b) evacuation for 8 min, $<8\times10^{-7}$ Torr, and (c) evacuation for 24 min, $<3\times10^{-7}$ Torr.

the second and forth are red-shifted by 6−8 cm^{-1}. It is most likely that the interaction between the methanol molecules at the first layer induces the shift of CH_3 vibrational frequency. The Fermi resonance at around 2910 cm^{-1} at the vapor/methanol interface is not obtained in our SFG spectra [30]. One possible reason could be that the feature is too small to be resolved.

The studies on single crystal rutile TiO_2(110) and anatase TiO_2(101) showed there were both molecular adsorption and dissociative adsorptionn of methoxy [8, 31]. Similar results were obtained on rutile TiO_2 nanoparticles [32]. There are several different sites for adsorption of methoxy on single crystal rutile TiO_2(110) and anatase TiO_2(101) from TPD studies [8, 31]. Here, we cannot distinguish methoxy groups at different sites from the vibrational frequency of CH_3. However, two types of methoxy groups were distinguished in our experiment, which had different photocatalytic reaction efficiencies under both aerobic and anaerobic conditions.

Based on the Eq.(1), the individual peak area equals $\pi A_q^2/\Gamma_q$, and the density of adsorbates (N) is proportional to $A_q(\pi/\Gamma_q)^{1/2}$. From our fitting results, both the densities of methoxy and molecular methanol on TiO_2 increase monotonically as the methanol pressure, as shown in Fig.5. The density ratios, $N_{\rm Res1}(\nu_{\rm s})/N_{\rm Res3}(\nu_{\rm F})$ and $N_{\rm Res4}(\nu_{\rm s})/N_{\rm Res4}(\nu_{\rm F})$, change as the methanol pressure, which might be ascribed to the complex Fermi-resonance interaction between the symmetric stretching and the bending-motion overtone [33–35]. Shultz and co-workers derived the adsorption energy of methoxy based on the Langmuir isotherm model [24]. But either Res1 or Res3 datum corresponding to methoxy deviates from the linearity between the methoxy quantity on TiO_2 and the inverse methanol pressure.

When we evacuated the cell after filling 300 Pa CH_3OH, the SFG peaks arising from molecular methanol largely decrease while the methoxy peaks are little affected, which is in accordance with the data of Shultz and co-workers [24]. Moreover, we found that further pumping out the cell results in the continuous decrease of the SFG signal of chemically adsorbed methoxy, as shown in Fig.6. The TPD results on TiO_2(110) show that the desorption temperature of methanol is around 295 K [8], so there is still some molecular methanol on the thin film at room temperature. DFT calculation showed that the adsorption energy of both methanol and its dissociated products, methoxy and H on BBO sites were almost degenerate, and the barrier was very low [13, 36, 37]. Thus, it is reasonable to assume that species including chemically adsorbed methoxy, molecular methanol, and the methanol in gas phase are dominated by the following equilibriums at room temperature:

$$CH_3OH(g) \rightleftarrows CH_3OH(a) \rightleftarrows CH_3O(a) + H(a) \qquad (2)$$

where the dissociation of methanol to methoxy equilibrates with the formation of methanol on surfaces, not directly with the methanol in the gas phase. It may

DOI:10.1063/1674-0068/28/cjcp1409154

interpret why the methoxy quantity does not obey the Langmuir isothermal model. According to the reaction (2), the methoxy and H on the surface can recombine to form CH_3OH and desorb subsequently, which is responsible for the decrease in SFG signal of chemically adsorbed methoxy as longer pumping out. The data show that this recombination rate is small at room temperature. Although methoxy on 5-coordianted Ti sites can recombine with the H on bridge-bonded oxygen sites on rutile $TiO_2(100)$ surface at 250 K, much lower than 300 K [14], and calculation also shows that the barrier of both dissociation and recombination of methanol 5-coordianted Ti sites are very small, about 0.2 eV [13, 36], methoxy groups adsorbed at variable sites on TiO_2 thin film, like step, kink, and point defect sites, may have high adsorption energy, which raises the recombination barrier and lowers the recombination rate.

IV. CONCLUSION

We describe a surface specific broadband infrared sum frequency generation vibrational spectrometer with third harmonic, 266 nm, excitation that has been newly set up in our laboratory for studying surface photocatalysis on surfaces. The *in situ* cleanup of surface contaminants was realized by photodegradation reactions in O_2 atmosphere. We measured the SFG vibrational spectrum of methanol on TiO_2 thin film in a differential pumping cell, and fit with a self-developed global fitting program. Both the molecular methanol and methoxy adsorption were identified with changing the methanol pressure, and the CH_3 symmetric stretching vibration frequency and Fermi resonance of molecular methanol is red-shifted by about 6−8 cm^{-1} from low to high coverage due to its interaction with the TiO_2 surface at the first layer. Obvious recombination between methoxy and H on TiO_2 surface was observed, which rate is small at the room temperature. Thus, we propose that two equilibriums exist: molecular methanol between in the gas phase and on the TiO_2 surface, and between molecular methanol and dissociative methanol on surfaces. The thin film surface is closer to the real applied material, but it is always too complicated to obtain more information at the atomic and molecular level due to its disorder and complexity. Therefore, the single crystal surface, which is well defined, is a good model to illuminate the adsorption and photocatalytic reaction details of organic molecules on TiO_2 surfaces.

Supplementary material: The fitting results of SFG spectra dependent on the methanol pressure are given.

V. ACKNOWLEDGMENTS

This work was supported by the National Basic Research Program of China (No.2013CB834600) and the National Natural Science Foundation of China (No.1127002/B030403, No.11290162/A040106, and No.21322310/B030402).

[1] A. Fujishima and K. Honda, Nature **238**, 37 (1972).
[2] M. A. Henderson, Surf. Sci. Rep. **66**, 185 (2011).
[3] C. L. Pang, R. Lindsay, and G. Thornton, Chem. Rev. **113**, 3887 (2013).
[4] C. L. Pang, R. Lindsay, and G. Thornton, Chem. Soc. Rev. **37**, 2328 (2008).
[5] X. Lang, W. Ma, C. Chen, H. Ji, and J. Zhao, Acc. Chem. Res. **47**, 355 (2013).
[6] H. Chen, C. E. Nanayakkara, and V. H. Grassian, Chem. Rev. **112**, 5919 (2012).
[7] Z. Dohnálek, I. Lyubinetsky, and R. Rousseau, Prog. Surf. Sci. **85**, 161 (2010).
[8] M. A. Henderson, S. Otero-Tapia, and M. E. Castro, Faraday Discuss. **114**, 313 (1999).
[9] Z. R. Zhang, O. Bondarchuk, J. M. White, B. D. Kay, and Z. Dohnálek, J. Am. Chem. Soc. **128**, 4198 (2006).
[10] M. Shen and M. A. Henderson, J. Phys. Chem. L **2**, 2707 (2011).
[11] K. Onda, B. Li, J. Zhao, and H. Petek, Surf. Sci. **593**, 32 (2005).
[12] C. Y. Zhou, Z. F. Ren, S. J. Tan, Z. B. Ma, X. C. Mao, D. X. Dai, H. J. Fan, X. M. Yang, J. LaRue, R. Cooper, A. M. Wodtke, Z. Wang, Z. Y. Li, B. Wang, J. L. Yang, and J. G. Hou, Chem. Sci. **1**, 575 (2010).
[13] Q. Guo, C. Xu, Z. Ren, W. Yang, Z. Ma, D. Dai, H. Fan, T. K. Minton, and X. Yang, J. Am. Chem. Soc. **134**, 13366 (2012).
[14] Q. Guo, C. Xu, W. Yang, Z. Ren, Z. Ma, D. Dai, T. K. Minton, and X. Yang, J. Phys. Chem. C **117**, 5293 (2013).
[15] K. R. Phillips, S. C. Jensen, M. Baron, S. C. Li, and C. M. Friend, J. Am. Chem. Soc. **135**, 574 (2012).
[16] Q. Yuan, Z. Wu, Y. Jin, L. Xu, F. Xiong, Y. Ma, and W. Huang, J. Am. Chem. Soc. **135**, 5212 (2013).
[17] B. Li, J. Zhao, K. Onda, K. D. Jordan, J. Yang, and H. Petek, Science **311**, 1436 (2006).
[18] A. Migani, D. J. Mowbray, A. Iacomino, J. Zhao, H. Petek, and A. Rubio, J. Am. Chem. Soc. **135**, 11429 (2013).
[19] A. Migani, D. J. Mowbray, J. Zhao, H. Petek, and A. Rubio, J. Chem. Theory Comput. **10**, 2103 (2014).
[20] M. A. Henderson, S. Otero-Tapia, and M. E. Castro, Surf. Sci. **412/413**, 252 (1998).
[21] M. Xu, Y. Gao, Y. Wang, and C. Woell, Phys. Chem. Chem. Phys. **12**, 3649 (2010).
[22] M. Xu, Y. Gao, E. M. Moreno, M. Kunst, M. Muhler, Y. Wang, H. Idriss, and C. Woell, Phys. Rev. Lett. **106**, (2011).
[23] G. A. Kimmel, M. Baer, N. G. Petrik, J. VandeVondele, R. Rousseau, and C. J. Mundy, J. Phys. Chem. L **3**, 778 (2012).

DOI:10.1063/1674-0068/28/cjcp1409154

[24] C. Y. Wang, H. Groenzin, and M. J. Shultz, J. Phys. Chem. B **108**, 265 (2004).
[25] C. Y. Wang, H. Groenzin, and M. J. Shultz, Langmuir **19**, 7330 (2003).
[26] L. Miao, P. Jin, K. Kaneko, A. Terai, N. Nabatova-Gabain, and S. Tanemura, Appl. Surf. Sci. **212/213**, 255 (2003).
[27] L. Velarde, X. Y. Zhang, Z. Lu, A. G. Joly, Z. M. Wang, and H. F. Wang, J. Chem. Phys. **135**, 241102-1 (2011).
[28] R. Lu, W. Gan, B. H. Wu, Z. Zhang, Y. Guo, and H. F. Wang, J. Phys. Chem. B **109**, 14118 (2005).
[29] Y. Yu, Y. Wang, K. Lin, N. Hu, X. Zhou, and S. Liu, J. Phys. Chem. A **117**, 4377 (2013).
[30] R. Superfine, J. Y. Huang, and Y. R. Shen, Phys. Rev. Lett. **66**, 1066 (1991).
[31] G. S. Herman, Z. Dohnálek, N. Ruzycki, and U. Diebold, J. Phys. Chem. B **107**, 2788 (2003).
[32] D. A. Panayotov, S. P. Burrows, and J. R. Morris, J. Phys. Chem. C **116**, 6623 (2012).
[33] R. G. Snyder and J. R. Scherer, J. Chem. Phys. **71**, 3221 (1979).
[34] R. G. Snyder, H. L. Strauss, and C. A. Elliger, J. Phys. Chem **86**, 5145 (1982).
[35] R. G. Snyder, A. L. Aljibury, H. L. Strauss, H. L. Casal, K. M. Gough, and W. F. Murphy, J. Chem. Phys. **81**, 5352 (1984).
[36] R. Sanchez de Armas, J. Oviedo, M. A. San Miguel, and J. F. Sanz, J. Phys. Chem. C **111**, 10023 (2007).
[37] J. Zhao, J. Yang, and H. Petek, Phys. Rev. B **80**, 235416 (2009).

DOI:10.1063/1674-0068/28/cjcp1409154